In situ monitoring of powder blending by non-invasive Raman spectrometry with wide area illumination

Pamela Allan,[a] Luke J. Bellamy,[a,1] Alison Nordon,[a]* David Littlejohn,[a]* John Andrews[b] and Paul Dallin[b]

[a] WestCHEM, Department of Pure and Applied Chemistry and CPACT, University of Strathclyde, 295 Cathedral Street, Glasgow, G1 1XL, UK

[b] Clairet Scientific Ltd., 17/18 Scirocco Close, Moulton Park Industrial Estate, Northampton, NN3 6AP, UK

[1] Present address: GlaxoSmithKline, Priory Street, Ware, SG12 0DJ, UK.

* denotes authors to whom correspondence should be sent

(Email: d.littlejohn@strath.ac.uk and alison.nordon@strath.ac.uk)

Abstract

A 785 nm diode laser and probe with a 6 mm spot size were used to obtain spectra of stationary powders and powders mixing at 50 rpm in a high shear convective blender. Two methods of assessing the effect of particle characteristics on the Raman sampling depth for microcrystalline cellulose (Avicel), aspirin or sodium nitrate were compared: (i) the information depth, based on the diminishing Raman signal of TiO_2 in a reference plate as the depth of powder prior to the plate was increased, and (ii) the depth at which a sample became infinitely thick, based on the depth of powder at which the Raman signal

This is an accepted author manuscript, accepted by Journal of Pharmaceutical and Biomedical Analysis, 04 December 2012.

of the compound became constant. The particle size, shape, density and/or light absorption capability of the compounds were shown to affect the "information" and "infinitely thick" depths of individual compounds. However, when different sized fractions of aspirin were added to Avicel as the main component, the depth values of aspirin were the same and matched that of the Avicel: 1.7 mm for the "information" depth and 3.5 mm for the "infinitely thick" depth. This latter value was considered to be the minimum Raman sampling depth when monitoring the addition of aspirin to Avicel in the blender. Mixing profiles for aspirin were obtained non-invasively through the glass wall of the vessel and could be used to assess how the aspirin blended into the main component, identify the end point of the mixing process (which varied with the particle size of the aspirin), and determine the concentration of aspirin in real time. The Raman procedure was compared to two other non-invasive monitoring techniques, near infrared (NIR) spectrometry and broadband acoustic emission spectrometry. The features of the mixing profiles generated by the three techniques were similar for addition of aspirin to Avicel. Although Raman was less sensitive than NIR spectrometry, Raman allowed compound specific mixing profiles to be generated by studying the mixing behaviour of an aspirin – aspartame – Avicel mixture.

< Take in Figure 1>

Keywords

Raman spectrometry; process analytical technologies (PAT); powder blending; sampling depth; real-time monitoring; pharmaceuticals.

1. Introduction

Raman spectrometry is proving to be a useful monitoring technique in the pharmaceutical industry, especially in secondary manufacturing [1, 2]. Considerable advantages have been demonstrated for analysis of tablets [3-18] and capsules [11, 19-23], particularly when transmission mode measurements were used [16-18, 20-24]. To ensure that pharmaceutical dosage forms contain the appropriate amount of active ingredient(s), the constituents must be blended to a homogeneous state. While transmission Raman spectrometry is suited for the analysis of tablets and capsules, the backscatter mode of measurement is more amenable for *in situ* analysis of larger unit operations such as powder blending. However, there are relatively few reports describing the use of backscatter Raman spectrometry for this purpose [25-27]; in contrast, use of *in situ* near infrared (NIR) spectrometry is far more common [28-33]. The mixing of diltiazem hydrochloride pellets and paraffinic wax was investigated by Vergote et al. using non-invasive Raman spectrometry [26]. The process was monitored via a glass window in the side of the vessel using a laser spot of approximately 2 mm diameter. There was no significant difference in the intensity of the Raman signal when the diltiazem pellets were stationary or mixing at 50 rpm. Therefore, spectra could be recorded without stopping the mixing procedure and the Raman signal became constant when homogeneity had been reached. De Beer et al. [25] monitored the blending of Avicel PH 102, lactose DCL 21, dilitazem hydrochloride, and silicium dioxide using an invasive Raman probe; the end of the probe was flush with the inner surface of the mixing vessel wall. The mixing end-point identified from the Raman measurements was comparable to that obtained using NIR spectrometry. Hausman et al. also reported the successful implementation of in-line

67 Raman spectrometry to monitor blending of azimilide dihydrochloride at low dose
68 (1% w/w) [27].

69 One reason for the limited application of Raman spectrometry to powder
70 processes is that conventional backscatter Raman systems typically employ optics that
71 produce laser spot sizes smaller than 500 μm diameter, which results in the measurement
72 of only a small volume of the sample. More representative sampling has been achieved
73 by continuously rotating a sample during measurement [5, 6, 9, 10, 13, 14, 34] or by
74 scanning at several positions [8, 34, 35], thereby increasing the sampling area. To
75 overcome some of the sub-sampling limitations of conventional backscatter Raman
76 systems, defocused probes or wide area sampling optics with laser beam diameters of 3 –
77 7 mm have also been investigated [15, 36-38]. Backscatter Raman measurements also
78 exhibit a strong bias towards the upper surface layers of the sample. Monte Carlo
79 simulations of the backscattered Raman signal from a 4 mm thick tablet using a 4 mm
80 diameter laser spot have shown that 88% of the signal is generated in the top 1 mm layer
81 of the tablet [24]. However, the increased sampling depth and area of wide area
82 illumination probes results in significantly larger sampling volumes compared to
83 conventional backscatter Raman probes. For example, it has been shown that Raman
84 signals can originate from material 13 mm below the surface of a sample with a PhAT
85 probe with a 7 mm spot size [38]. The sampling volume of a PhAT probe (3 mm spot
86 size) was found to be approximately 1300 times larger than that of a non-contact Raman
87 probe (150 μm spot size) and approximately 16700 times larger than that of an
88 immersion probe (60 μm spot size) [36]. The larger sampling volume associated with the
89 PhAT probe resulted in comparable results to NIR spectrometry for quantification of

mixtures of anhydrous and hydrated polymorphs; the sampling volume of the PhAT probe was found to be comparable to that for the NIR probe [39]. When mixtures of polymorphs of flufenamic acid (forms I and III) with different particle sizes were analysed using large and small spot size Raman probes, the wide area illumination probe was found to be less sensitive to particle size owing to the larger sampling volume measured with this probe [37].

This report describes the first use of a PhAT probe for *in situ* Raman monitoring of powder mixing in a high shear blender. The study included evaluation of the effect of particle size variations on the sampling depth that can be achieved with the PhAT probe to allow comparison with previously reported results obtained with probes of different optical configurations. In addition, the effect of particle size on the Raman signal was investigated; this was important as the effect of particle size on the backscatter Raman signal is highly dependent on the optical configuration of the probe employed [40]. Mixing profiles based on non-invasive Raman spectrometry have been assessed to compare the information they provide with mixing profiles produced by non-invasive NIR spectrometry and broadband acoustic emission (AE) spectrometry. Some advantages of Raman measurements over NIR spectrometry were identified for powder monitoring.

2. Experimental

2.1. Instrumentation

2.1.1. Raman spectrometer

A Kaiser Raman RXN1 spectrometer with a PhAT probe (Kaiser Optical Systems Inc., Ann Arbor. MI, USA) was used for all experiments except where stated below. The 785 nm Invictus diode laser was operated at 400 mW at source. The laser beam was optically expanded to give a 6 mm spot size, a working distance of 254 mm and a depth of field of 50 mm. The probe to sample distance was 203 mm. For the sampling depth studies, spectra were acquired using an exposure time of 0.5 s and 1 accumulation. *In situ* Raman measurements were made through the glass wall of the mixing vessel during the powder blending experiments. A spectrum was acquired every 5 s with an exposure time of 2.5 s and 1 accumulation. The exposure time for each set of experiments was selected such that the largest Raman signal occupied approximately 60 – 70% of the dynamic range of the CCD detector.

For the experiment comparing Raman, NIR and AE, and the monitoring of the blending of a three component mixture, a different PhAT probe system was used. In this case, the 785 nm laser beam was optically expanded to give a 3 mm spot size and a working distance of 100 mm. The probe to sample distance was 100 mm. Spectra were acquired every 3 s, through the wall of the vessel, with an exposure time of 2 s and 1 accumulation.

A spectrum of aspartame was acquired using a Kaiser RXN1 spectrometer with a MR probe equipped with a non-contact optic (0.4 inch working distance and a laser spot

size of approximately 100 μm). An Invictus diode laser with a wavelength of 785 nm was employed, and was operated at 350 mW at the source. Aspartame was contained within a glass sample vial, which was placed in the off-line sample compartment, and the spectrum was acquired through the side of the vial using an exposure time of 4.0 s and 1 accumulation.

Data were acquired using HoloGRAMS software (Kaiser Optical Systems). A dark current spectrum was obtained before each set of experiments and subtracted automatically from each subsequent spectrum acquired. Data were exported into GRAMS/32 and converted to text files, which were subsequently imported into Matlab 7.0 (Mathworks Inc., Natick, Massachusetts, USA) for analysis using the PLS_Toolbox version 3.04 (Eigenvector Research Inc., Manson, Washington, USA). As spectra of samples containing Avicel exhibited a sloping baseline arising from fluorescence, second derivative spectra were calculated throughout using the Savitzky – Golay function with a second order polynomial and a 13 or 25 point filter width for data acquired using the 6 or 3 mm laser spot size, respectively.

2.1.2. Near infrared reflectance spectrometer

Some measurements of powder mixing were obtained simultaneously by non-invasive Raman spectrometry, NIR spectrometry and broadband AE spectrometry. *In situ* NIR measurements were made through the glass wall of the vessel as described previously [31, 32] using a Zeiss Corona 45 NIR spectrometer (Carl Zeiss, Heidenheim, Germany). Measurements were acquired using Aspect software (Carl Zeiss) package and spectra stored as log(1/R) where R is the reflectance and was calculated from the intensity of light reflected by the sample relative to that for a reflectance standard. The integration

time was 32 ms and 10 scans were co-added for each acquired spectrum allowing measurements to be taken every 0.5 s. Data were exported as text files into Matlab for further analysis using PLS_Toolbox. First derivative spectra were calculated using the Savitzky – Golay function with a 5 point filter width and second order polynomial.

2.1.3. Acoustic emission

The broadband AE monitoring equipment has been described previously [41]. A Nano 30 transducer (Physical Acoustics Ltd, Cambridge, UK) was attached to the glass wall of the mixing vessel using a silicone-based vacuum grease (Dow Corning) and adhesive tape. The Nano 30 transducer was attached to a 2/4/6 series pre-amplifier (Physical Acoustics Limited). The pre-amplifier required a 28 V power supply (Physical Acoustics Limited) and the gain of the pre-amplifier was set to 60 dB. The pre-amplifier was connected to an Agilent 54642A oscilloscope using a 5 m length cable, which was linked to a computer via a GPIB to USB interface (Agilent Technologies).

A data capture program, written in C^{++} by Douglas McNab and Robbie Robinson from the Centre of Ultrasonic Engineering (CUE) at the University of Strathclyde, enabled the cyclic sampling of the acoustic signals displayed on the oscilloscope and signals were saved as comma separated variable (CSV) files. Signals were acquired using a sampling rate of 2 MHz and the time interval between collection of signals was 2 s. A total of 450 signals were collected with each signal consisting of 4000 points. All acoustic signals were imported into Matlab for analysis. A power spectrum was calculated of each signal and three spectra were co-added to give a composite spectrum every 6 s. Signal areas were calculated by summing the intensities of the signals between 0 and 400 kHz.

176

177 **2.2. Powders**

178 Microcrystalline cellulose (Avicel PH-101; FMC, Cork, Ireland), aspirin, sodium nitrate
179 (both from Sigma-Aldrich, Dorset, UK) and aspartame (provided by GSK, UK) were
180 used. The Avicel particles have a tap density of 0.45 g cm^{-3}, are granular in shape and
181 have an average particle size of 50 μm. Aspirin particles are low aspect ratio needles with
182 an average particle size of 192 μm. Sodium nitrate particles are granular with an average
183 particle size of 275 μm. Aspartame particles are high aspect needles (particle size was not
184 measured). Average particle size information was obtained by laser diffraction, while
185 density and shape information was obtained from the literature [42]. The powders were
186 sieved through 10 cm diameter brass pan sieves (Endecotts Ltd, UK) to obtain different
187 particle size ranges: <38, 38 – 53, 53 – 106, 150 – 212, 212 – 250, 250 – 300, 300 – 355
188 and 355 – 425 μm for Avicel; <106, 106 – 150, 212 – 250, 250 – 300, 300 – 355, and 425
189 – 500 μm for aspirin; 150 – 212, 212 – 250, 250 – 300, 300 – 355, 355 – 425, 425 – 500
190 and 500 – 800 μm for sodium nitrate. The mid-point of the sieve range has been used in
191 plots to represent each particle size fraction.

192

193 **2.3. Procedures**

194 **2.3.1. Raman sampling depth studies**

195 A 2.68 mm thick layer of glass was placed on top of the inverted PhAT probe with a
196 203 mm spacer attached (Figure 1a). A series of plastic plates, with a 30 mm diameter
197 hole, were placed on top of the glass plate (Figures 1b and 1c). For investigation of

198 powder depths of 0 – 4.48 mm, up to 16 × 0.28 mm thick plates were stacked on top of
199 each other. A depth of 8.48 mm was obtained by placing an additional 4 mm thick plastic
200 plate on top of the 16 plates. This combination of plates enabled sampling depths of
201 ≤4.48 mm to be measured. The powder was carefully placed into the hole in the plastic
202 plates and levelled off using a razor blade, ensuring minimal compaction of the solid, and
203 the mass of solid was recorded. A TiO_2 reference layer (solid particles of TiO_2 sealed
204 between two microscope slides) was placed over the top layer of the powder (Figures 1b
205 and 1c) with aluminium foil used as the final layer to reduce loss of laser and Raman
206 photons from the upper surface of the TiO_2 reference layer. Each corner of the
207 microscope slide was labelled to ensure consistency in positioning, so that the same part
208 of the TiO_2 was analysed each time. A spirit level was placed on top of the glass above
209 the spectrometer to ensure the radiation was pointing vertically upwards (see Figure 1a).
210 Analysis of the variance of the Avicel signal at 1095 cm^{-1} revealed that the repeatability
211 (expressed as the relative standard deviation (RSD) for n = 6) of the Raman
212 measurements, positioning of the sample holder, the weighing procedure and the powder
213 levelling process were 0.22, 0.34, 0.66, and 0.26%, respectively.

214 The information depth was estimated using the TiO_2 Raman signal at 397 cm^{-1}. As
215 the depth of Avicel, aspirin or sodium nitrate increased, the TiO_2 signal decreased until it
216 became zero; hence, the information depth was defined as the point where the exciting
217 laser can no longer penetrate the powder to generate a detectable Raman signal of the
218 TiO_2 reference layer. This type of approach has been used previously for information
219 depth measurements in NIR reflectance spectrometry [31, 43, 44]. A second set of
220 measurements was made based on the change in the intensity of the Raman signals of

Avicel, aspirin and sodium nitrate powders at 1095, 1606 and 1068 cm^{-1}, respectively. In this case, the Raman signal increases with powder depth and then becomes constant, which defines the depth of powder at which the sample effectively becomes infinitely thick. These measurements were made to allow comparisons with the results of previous Raman studies [36, 40] and a study on reflectance NIR which used a similar protocol to assess the sampling depth for aspirin powders [31].

2.3.2. Powder blending

The scaled-down convective mixer has been described previously [31, 32, 41]. The vessel has a pot size of about 500 mL, a radius of 4 cm and is made of glass. The impeller has three blades set 120° apart with a tilt angle of 45°; each blade is approximately 29 mm long and 12 mm wide. Powders were mixed at 50 rpm using a stirrer motor (IKA Eurostar, VWR International).

For the mixing of two components, 75 g of unsieved Avicel PH-101 was placed into the vessel and mixed. After 120 s, different masses (0, 5, 10, 20, 30 or 40 g) of either unsieved or size fractions of sieved aspirin (<106, 250 – 300 or 425 – 500 μm) were added via a funnel positioned directly above the centre of the vessel and the powders were allowed to mix for a further 780 s. A further experiment was also conducted in which 25 g of unsieved aspirin and 25 g of unsieved aspartame was added to 75 g of unsieved Avicel PH-101 after 120 and 900 s, respectively; the total mixing time was 2100 s.

3. Results and Discussion

3.1. Raman spectra

Individual Raman spectra of aspirin, Avicel, and sodium nitrate measured through a glass plate, aspartame measured through the wall of a glass vial, the TiO_2 reference layer, and the glass plate are illustrated in Figure 2. The Raman spectrum of TiO_2 contains peaks at approximately 143, 397, 520 and 640 cm^{-1}, indicating that the TiO_2 is predominantly in the anatase phase [45]. The broad peak that appears at approximately 1400 cm^{-1} in all spectra in Figure 2 can be attributed to the glass plate.

The TiO_2 peak at 397 cm^{-1} was least affected by the other compounds and so was used for the information depth experiments. The peaks at 1068 and 1606 cm^{-1} in the sodium nitrate and aspirin spectra, respectively, were used to determine the depth at which the sample becomes infinitely thick. A small peak in the Avicel spectrum at approximately 1095 cm^{-1} was also measured, but was found to have poor sensitivity compared to the peaks selected for the other two compounds.

3.2. Raman information depths for uncompacted powders

A number of particle size ranges of Avicel, aspirin and sodium nitrate were analysed at increasing depths using the set-up illustrated in Figure 1, and the second derivative Raman spectral intensities were recorded. When the TiO_2 peak at 397 cm^{-1} could no longer be detected, the depth of the selected powder was deemed to be the information depth limit. Figure 3 gives a summary of the information depths for the different particle size fractions of each compound. In each case, the information depth increased with

particle size before becoming constant at higher particle sizes. As the information depth for 300 – 355 μm aspirin and 355 – 425 μm sodium nitrate particles was found to be >4.48 mm and so could not be determined, values for these fractions were not included in Figure 3. The increase in information depth with particle size is consistent with Kubelka-Munk theory. Diffuse reflectance decreases as particle size increases [46, 47] and consequently, the exciting laser intensity and the Raman signal generated can propagate through larger depths of powder. The differences in information depth for similar sizes of Avicel, aspirin and sodium nitrate particles <400 μm indicates that the particle shape, density and/or the light absorption capability of the compounds affect the depth of powder through which the TiO_2 Raman spectrum can be measured.

As the intention was to use the PhAT probe to monitor powder blending in a mixer, information depths for TiO_2 at 397 cm^{-1} were obtained for 10, 30 and 40 g of aspirin blended with 75 g Avicel PH-101 to give aspirin concentrations of 11.8, 28.6 and 34.8% w/w, respectively. Three particle size ranges of aspirin were used: <106, 250 – 300 and 425 – 500 μm. The information depth for each of the mixtures was in the range 1.7 – 2.0 mm, similar to the value for unsieved Avicel PH-101 (1.7 mm). These findings are similar to those obtained using NIR spectrometry, i.e. the information depth for the analyte compound is determined by the main component in the mixture [31].

3.3. Depth of powder at which sample becomes infinitely thick

The depth of powder at which the 2nd derivative Raman signal of Avicel (1095 cm^{-1}), aspirin (1606 cm^{-1}) or sodium nitrate (1068 cm^{-1}) became constant was different for each compound and varied with particle size. The depth was found to be >3 mm for each

287 particle size range for Avicel. For sodium nitrate, the depth for the two smallest fractions
288 (150 – 212 μm and 212 – 250 μm) was about 0.8 – 1 mm, whereas for the other particle
289 sizes, the value was 3.5 – 3.9 mm. For aspirin, the depth initially increased with
290 increasing particle size (from 3.8 to 4.5 mm) then decreased to 3.5 mm for the largest
291 aspirin particle size range (425 – 500 μm) analysed. When other peaks in the aspirin
292 spectrum (292, 751 and 1045 cm^{-1}) were measured, the information depth values were no
293 different to those obtained at 1606 cm^{-1}. In contrast, it has been shown that different
294 peaks in the NIR spectrum of aspirin give different "infinitely thick" sample depths
295 owing to the different absorptivities of the first and second overtones in the spectrum (0.6
296 – 1.1 mm and 1.1 – 2.2 mm, respectively, depending on particle size) [31].

297 Wang et al. [40] investigated the effect of particle characteristics on the Raman
298 sampling depth for a number of crystalline powders using the "infinitely thick" method
299 and found similar trends to those reported here. An increase in sampling depth was
300 observed with average particle size in the range 108 – 428 μm for sodium nitrate;
301 however, the values obtained (6 – 15.5 mm) were much larger than those obtained in the
302 present study. This is likely to be due to a combination of factors; the laser wavelength
303 (514.5 nm) was shorter (sampling depth is wavelength dependent [48]) and a different
304 optical configuration was employed, which has a strong influence on the sampling depth
305 [40]. The sampling depth of a prototype Raman PhAT probe with a 3 mm diameter laser
306 spot size was reported to be 2 mm for theophylline discs, using the "infinitely thick"
307 method [36]. However, it has been shown that the sampling depth is less for pressed
308 material compared to uncompacted powders [40].

When the previously mentioned particle size fractions of aspirin were mixed with unsieved Avicel, the intensity of the aspirin peak at 1606 cm^{-1} became constant at a depth of 3.5 – 3.9 mm for all the mixtures. This indicates that similar to the information depth measurements, the depth at which an infinitely thick sample is achieved is influenced principally by the main component and is less affected by particle size variations of the minor component. If the sampling depth is 3.5 mm for mixtures of Avicel and aspirin and it is assumed that all layers within the 3.5 mm contribute equally to the Raman signal, then with a 6 mm diameter laser spot the sampling volume is 99.0 mm^3. This equates to a mass of 0.045 g if the density (tap) of the powder is assumed to be that of Avicel (0.45 g cm^{-3}). However, it can be estimated from the information depth plots that approximately 90% of the Raman signal is generated in the upper 1 mm layer of the powder; this is consistent with the results of Monte Carlo simulations by Matousek and Parker [24]. Therefore, the mass of sample that contributes to approximately 90% of the Raman signal is 0.013 g.

The depth at which a sample becomes infinitely thick is generally greater than the information depth determined using a reference layer of TiO_2. When a reference layer is used, the laser photons propagate through the powder to the reference layer where Raman photons of the reference material are generated. The backscattered Raman photons then propagate back through the powder where they are detected. Consequently, the Raman signal used to determine the information depth is only generated in the plane of the reference layer. In comparison, when a compound peak is used Raman photons can be generated throughout the entire depth of the powder. In such situations, the Raman signal decays slower than the exciting laser intensity [49, 50] and so it might be expected that

the sampling depth determined using this method will be greater. As the infinitely thick depth is determined using a signal from the sample powder, this will reflect more accurately the depth of material sampled by the Raman probe during powder blending.

3.4. Effect of particle size on Raman intensities

The second derivative Raman intensity of aspirin, Avicel and sodium nitrate was measured for each particle size range with a powder depth of 8.48 mm, well in excess of the depth required to achieve an infinitely thick sample for each compound (see Figure 4). The aspirin peak intensity at 1606 cm^{-1} increases then decreases with increasing particle size, with the maximum (i.e. largest negative) signal intensity occurring at the intermediate particle size ranges. A similar trend was observed for the sodium nitrate and Avicel peak intensities at 1068 and 1095 cm^{-1}, respectively.

Kubelka-Munk theory states that diffuse reflectance increases as particle size decreases, which limits the volume of sample contributing to the Raman signal, and therefore, the Raman intensity should increase with increasing particle size [46, 47]. The Raman signals for aspirin, sodium nitrate and Avicel increase with particle size at lower particle sizes, in accordance with Kubelka-Munk theory; however, the signal decreases with an increase in particle size for larger particles. A similar trend to that observed in Figure 4 was observed in an earlier study by Wang et al. [40], when the probe to sample distance was increased to 10 mm to increase the unfocused spot diameter illuminating the sample to ~ 5 mm, and also by Hu et al. [37] when monitoring different particle sizes of flufenamic acid (form I) with small sampling volume probes (0.25 and 0.5 inch diameter immersion optics with a 60 μm laser spot size). In both of these studies, the maximum

Raman signal intensity was observed for most samples in the intermediate particle size range [37, 40]. Although the variation in intensity with particle size predicted by Kubelka-Munk theory was not observed experimentally in a number of studies [37, 40, 51], Wang et al. [40] demonstrated that there was a strong correlation between the Raman intensity and diffuse reflectance. The main reason for the difference is that Kubelka-Munk theory assumes confocal excitation and collection, but in the absence of diffuse reflectance it is likely that the optical configurations employed in the experimental studies had incomplete overlap of the collection and excitation cones. So while an increase in diffuse reflectance decreases the sampling depth, it also increases lateral spreading of the exciting laser beam. This generates additional Raman photons in the region of the collection fibre, which caused an increase in the Raman signal with a decrease in particle size observed in studies by Wang et al. (with a 0.5 mm laser spot size and a probe to sample distance of 1 mm) [40] and by Pellow-Jarman et al. [51]. When the probe to sample distance was increased in the study by Wang et al. [40] (as discussed above), there was greater overlap between the collection and excitation cones and so the improved overlap of the two cones caused by lateral spreading of the excitation beam is less important; hence, the different trends observed at the two different sample to probe distances (and beam diameters).

It is apparent that the variation in Raman signal observed with particle size is highly dependent on the optical arrangement employed [40]; it is a balance between signal enhancement through lateral spreading of the beam and signal reduction through a decrease in the sampling depth caused by diffuse reflectance. The PhAT probe mainly used in the present study (6 mm laser beam diameter), has good overlap of the excitation

and collection cones because of very weak divergence of the beam (i.e. close to a collimated beam with a large depth of field of approximately ±1 inch) [52]. Consequently, signal enhancement by the lateral beam spreading is less important and so the signal intensity is correlated to the sampling depth (as predicted by Kubelka-Munk theory) up to a certain particle size. For larger particle sizes, it may be that Raman photons are emitted outwith the collection volume of the PhAT probe owing to the greater propagation distances.

3.5. Powder Blending

Different masses and particle sizes of aspirin were added to 75 g Avicel PH-101 as it was agitated in the mixer. Example second derivative spectra obtained during the mixing of 40 g of 250 – 300 μm aspirin particles and Avicel PH-101 are shown in Figure 5; aspirin was added to the Avicel at 120 s. The Raman intensities of the aspirin peaks in the measured spectra increased as the mass of the aspirin was increased and correspondingly the Avicel peak intensity decreased. Mixing profiles were produced by plotting the second derivative Raman intensity against time for the aspirin peaks at 751 and 1606 cm^{-1}. The same trends were noted for measurements at each peak so only the results based on 1606 cm^{-1} are discussed. The mixing profiles for addition of 0 – 40 g of the 250 – 300 μm aspirin particles are shown in Figure 6. On addition of aspirin after 120 s, a large increase in Raman scattering occurred at 1606 cm^{-1} as a result of the mixing properties of the mixer, whereby the aspirin powder is drawn down towards the bottom of the vessel and then up the side of the vessel through the Raman observation zone. As mixing continued, the 2nd derivative signal of aspirin became less negative as the mixture

401 became homogenous, with the larger masses of aspirin taking longer to achieve a more
402 constant plateau signal.

403 The mixing profiles for the other two particle sizes of aspirin were similar to those
404 in Figure 6, however, the time taken to achieve a homogeneous mixture and the variation
405 (peak-to-peak noise) of the profile at the plateau region increased with particle size for
406 each mass of aspirin added. Bellamy et al. [31] obtained similar mixing profiles to those
407 reported here when non-invasive NIR spectrometry was used to monitor the addition of
408 aspirin to Avicel PH-101 in the same type of mixer. The lesser variability in the Raman
409 profile signal at the plateau region when mixing smaller aspirin particles is due to the
410 more consistent number of aspirin particles passing through the measurement region at
411 any time than occurs for mixing of larger particle sizes; a similar phenomenon was
412 observed by Bellamy et al. [31] for the NIR-based mixing profiles. The magnitude of the
413 mean Raman signal in the plateau region at 700 – 900 s was calculated for each of the
414 mixing profiles and plotted against the mass of aspirin added. A linear response curve
415 was generated for each particle size range of aspirin with slopes of -0.278 (R^2 =
416 0.986), -0.329 (R^2 = 0.998), and -0.312 (R^2 = 0.997) obtained for <106, 250 – 300 and
417 425 – 500 μm particles, respectively. The lesser sensitivity obtained with the <106 μm
418 particles is probably related to the different shape of these particles (more granular than
419 needle-shaped) identified from microscope images. It is likely that with the large
420 sampling volume used in this study, the change in the relative number of particles with
421 aspirin particle size becomes less significant and so the spectrum obtained is still
422 representative of the mass fraction of aspirin [37]. The estimated sampling volume with a
423 mixing speed of 50 rpm and a sampling depth of 3.5 mm is 11095 mm^3 (assuming all

424 layers contribute equally), which equates to a mass of 4.99 g. However, if 90% of the
425 Raman signal is generated in the top 1 mm layer of powder, then most of the measured
426 signal arises from 1.43 g of sample.

427 The NIR method of Bellamy et al. [31] and a previously reported procedure for
428 monitoring powder blending by broadband acoustic emission spectrometry [41] were
429 used simultaneously with Raman spectrometry to compare the mixing profiles obtained
430 by the three non-invasive techniques. Example profiles are given in Figure 7 for addition
431 of 30 g aspirin to 75 g Avicel PH-101 mixing at 50 rpm. The features of the mixing
432 profiles, including the end-point of blending to a homogeneous mixture, were similar for
433 the three techniques, although the signal to noise was best for NIR and poorest for
434 acoustic emission. De Beer et al. [25] also found in-line Raman and NIR spectrometry
435 produced similar end-points (defined by the content uniformity method [30]) when used
436 simultaneously to monitor mixing of Avicel PH-102, lactose DCL 21 and silicium
437 dioxide in a high shear blender. However, there is clearer correspondence between the
438 mixing profiles over the entire blending experiment in the present study, as the mixing
439 profiles were derived from the spectral signals related to the added component and the
440 spectral measurements were acquired at a higher acquisition frequency. Table 1 gives a
441 comparison of the detection limit for unsieved aspirin mixing at 50 rpm in unsieved
442 Avicel PH101 for non-invasive NIR spectrometry, Raman spectrometry, and acoustic
443 emission. The detection limit calculated for Raman measurements was about an order of
444 magnitude poorer than that obtained with NIR spectrometry with a Zeiss Corona
445 instrument, but 5-fold better than the value obtained for acoustic emission with a Nano30
446 transducer.

447 Raman measurements were also obtained for addition of 25 g aspirin (after 120 s)
448 and then 25 g aspartame (after 900 s) to 75 g of Avicel PH-101. Inspection of the second
449 derivative spectra of the compounds revealed that mixing profiles could be plotted based
450 on well resolved peaks for aspirin or aspartame with minimal interference from the other
451 compounds; this is an advantage over NIR spectrometry for monitoring multiple
452 component systems where multivariate techniques are generally needed to deconvolute
453 the relative contributions from each compound. Example Raman mixing profiles based
454 on the aspirin peak at 1606 cm^{-1} and the aspartame peak at 1006 cm^{-1} are shown in Figure
455 8. As observed in Figure 6, on addition of aspirin to the mixer at 120 s, there was an
456 initial large increase in the aspirin signal, which then decreased to a constant value; as
457 expected, the aspartame response remained at approximately zero when aspirin was
458 added to the Avicel. However, on addition of aspartame to the vessel at 900 s, there was a
459 large change in the aspartame signal at about 1000 s. The oscillating mixing profile of
460 aspartame between 1200 and 1600 s is characteristic of a cohesive particle [32]. The
461 aspirin signal was affected by the addition of aspartame, initially increasing slightly
462 owing to minor compaction of the powder mixture in the vessel followed by a reduction
463 owing to dilution of the aspirin concentration as aspartame is blended in to the mixture.

464

465 ## 4. Conclusions

466 This study has shown that non-invasive Raman spectrometry with an optically broadened
467 spot size of 6 mm gives sampling depths of over 3 mm for measurement of aspirin in
468 Avicel; this is greater than the value obtained for non-invasive NIR spectrometry in a
469 previous study [31]. *In situ* Raman measurements can be used to produce mixing profiles

to study how the powders mix together, identify when the end point of mixing has occurred, and perform quantitative analysis in real time. Although less sensitive than a previously reported non-invasive NIR procedure, the Raman method could offer advantages when optimising mixing regimes for multi-component samples, as it may allow individual compound specific mixing profiles to be produced because of the technique's greater chemical specificity.

Acknowledgements

The support of EPSRC/DTI through LINK grant GR/R/19366/01 is acknowledged. CPACT is thanked for funding PA and LJB's PhD studentships, and the Royal Society is thanked for the award of a University Research Fellowship to AN.

References

[1] J. Rantanen, Process analytical applications of Raman spectroscopy, J. Pharm. Pharmacol., 59 (2007) 171-177.

[2] T. De Beer, A. Burggraeve, M. Fonteyne, L. Saerens, J.P. Remon, C. Vervaet, Near infrared and Raman spectroscopy for the in-process monitoring of pharmaceutical production processes, Int. J. Pharm., 417 (2011) 32-47.

[3] M. Dyrby, S.B. Engelsen, L. Nørgaard, M. Bruhn, L. Lundsberg-Nielsen, Chemometric quantitation of the active substance (containing C N) in a pharmaceutical tablet using near-infrared (NIR) transmittance and NIR FT-Raman spectra, Appl. Spectrosc., 56 (2002) 579-585.

[4] C.G. Kontoyannis, Quantitative determination of $CaCO_3$ and glycine in antacid tablets by laser Raman spectroscopy, J. Pharm. Biomed. Anal., 13 (1995) 73-76.

[5] R. Szostak, S. Mazurek, FT-Raman quantitative determination of ambroxol in tablets, J. Mol. Struct., 704 (2004) 229-233.

[6] R. Szostak, S. Mazurek, Quantitative determination of acetylsalicylic acid and acetaminophen in tablets by FT-Raman spectroscopy, Analyst, 127 (2002) 144-148.

[7] L.S. Taylor, F.W. Langkilde, Evaluation of solid-state forms present in tablets by Raman spectroscopy, J. Pharm. Sci., 89 (2000) 1342-1353.

501 [8] G.J. Vergote, C. Vervaet, J.P. Remon, T. Haemers, F. Verpoort, Near-infrared FT-
502 Raman spectroscopy as a rapid analytical tool for the determination of diltiazem
503 hydrochloride in tablets, Eur. J. Pharm. Sci., 16 (2002) 63-67.

504 [9] C. Wang, T.J. Vickers, C.K. Mann, Direct assay and shelf-life monitoring of aspirin
505 tablets using Raman spectroscopy, J. Pharm. Biomed. Anal., 16 (1997) 87-94.

506 [10] H. Wikström, S. Romero-Torres, S. Wongweragiat, J.A.S. Williams, E.R. Grant,
507 L.S. Taylor, On-line content uniformity determination of tablets using low-resolution
508 Raman spectroscopy, Appl. Spectrosc., 60 (2006) 672-681.

509 [11] S. Mazurek, R. Szostak, Quantitative determination of diclofenac sodium in solid
510 dosage forms by FT-Raman spectroscopy, J. Pharm. Biomed. Anal., 48 (2008) 814-821.

511 [12] S.E.J. Bell, D.T. Burns, A.C. Dennis, L.J. Matchett, J.S. Speers, Composition
512 profiling of seized ecstasy tablets by Raman spectroscopy, Analyst, 125 (2000) 1811-
513 1815.

514 [13] S. Mazurek, R. Szostak, Quantitative determination of captopril and prednisolone in
515 tablets by FT-Raman spectroscopy, J. Pharm. Biomed. Anal., 40 (2006) 1225-1230.

516 [14] M.G. Orkoula, C.G. Kontoyannis, Non-destructive quantitative analysis of
517 risperidone in film-coated tablets, J. Pharm. Biomed. Anal., 47 (2008) 631-635.

518 [15] M. Kim, H. Chung, Y. Woo, M. Kemper, New reliable Raman collection system
519 using the wide area illumination (WAI) scheme combined with the synchronous intensity

520 correction standard for the analysis of pharmaceutical tablets, Anal. Chim. Acta, 579
521 (2006) 209-216.

522 [16] J. Johansson, A. Sparén, O. Svensson, S. Folestad, M. Claybourn, Quantitative
523 transmission Raman spectroscopy of pharmaceutical tablets and capsules, Appl.
524 Spectrosc., 61 (2007) 1211-1218.

525 [17] M. Fransson, J. Johansson, A. Sparén, O. Svensson, Comparison of multivariate
526 methods for quantitative determination with transmission Raman spectroscopy in
527 pharmaceutical formulations, J. Chemom., 24 (2010) 674-680.

528 [18] A. Sparén, J. Johansson, O. Svensson, S. Folestad, M. Claybourn, Transmission
529 Raman spectroscopy for quantitative analysis of pharmaceutical solids, Am. Pharm. Rev.,
530 12 (2009) 62-71.

531 [19] J. Kim, J. Noh, H. Chung, Y.-A. Woo, M.S. Kemper, Y. Lee, Direct, non-destructive
532 quantitative measurement of an active pharmaceutical ingredient in an intact capsule
533 formulation using Raman spectroscopy, Anal. Chim. Acta, 598 (2007) 280-285.

534 [20] C. Eliasson, N.A. Macleod, L.C. Jayes, F.C. Clarke, S.V. Hammond, M.R. Smith, P.
535 Matousek, Non-invasive quantitative assessment of the content of pharmaceutical
536 capsules using transmission Raman spectroscopy, J. Pharm. Biomed. Anal., 47 (2008)
537 221-229.

538 [21] P. Matousek, A.W. Parker, Non-invasive probing of pharmaceutical capsules using
539 transmission Raman spectroscopy, J. Raman Spectrosc., 38 (2007) 563-567.

[22] K. Buckley, P. Matousek, Recent advances in the application of transmission Raman spectroscopy to pharmaceutical analysis, J. Pharm. Biomed. Anal., 55 (2011) 645-652.

[23] M.D. Hargreaves, N.A. Macleod, M.R. Smith, D. Andrews, S.V. Hammond, P. Matousek, Characterisation of transmission Raman spectroscopy for rapid quantitative analysis of intact multi-component pharmaceutical capsules, J. Pharm. Biomed. Anal., 54 (2011) 463-468.

[24] P. Matousek, A.W. Parker, Bulk Raman analysis of pharmaceutical tablets, Appl. Spectrosc., 60 (2006) 1353-1357.

[25] T.R.M. De Beer, C. Bodson, B. Dejaegher, B. Walczak, P. Vercruysse, A. Burggraeve, A. Lemos, L. Delattre, Y.V. Heyden, J.P. Remon, C. Vervaete, W.R.G. Baeyens, Raman spectroscopy as a process analytical technology (PAT) tool for the in-line monitoring and understanding of a powder blending process, J. Pharm. Biomed. Anal., 48 (2008) 772-779.

[26] G.J. Vergote, T.R.M. De Beer, C. Vervaet, J.P. Remon, W.R.G. Baeyens, N. Diericx, F. Verpoort, In-line monitoring of a pharmaceutical blending process using FT-Raman spectroscopy, Eur. J. Pharm. Sci., 21 (2004) 479-485.

[27] D.S. Hausman, R.T. Cambron, A. Sakr, Application of Raman spectroscopy for on-line monitoring of low dose blend uniformity, Int. J. Pharm., 298 (2005) 80-90.

[28] S.S. Sekulic, H.W. Ward, D.R. Brannegan, E.D. Stanley, C.L. Evans, S.T. Sciavolino, P.A. Hailey, P.K. Aldridge, On-line monitoring of powder blend homogeneity by near-infrared spectroscopy, Anal. Chem., 68 (1996) 509-513.

561 [29] O. Berntsson, L.G. Danielsson, B. Lagerholm, S. Folestad, Quantitative in-line
562 monitoring of powder blending by near infrared reflection spectroscopy, Powder
563 Technol., 123 (2002) 185-193.

564 [30] C. Bodson, W. Dewe, P. Hubert, L. Delattre, Comparison of FT-NIR transmission
565 and UV-vis spectrophotometry to follow the mixing kinetics and to assay low-dose
566 tablets containing riboflavin, J. Pharm. Biomed. Anal., 41 (2006) 783-790.

567 [31] L.J. Bellamy, D. Littlejohn, A. Nordon, Real-time monitoring of powder mixing in a
568 convective blender using non-invasive reflectance NIR spectrometry, Analyst, 133
569 (2008) 58-64.

570 [32] L.J. Bellamy, A. Nordon, D. Littlejohn, Effects of particle size and cohesive
571 properties on mixing studied by non-contact NIR, Int. J. Pharm., 361 (2008) 87-91.

572 [33] D. Ely, S. Chamarthy, M.T. Carvajal, An investigation into low dose blend
573 uniformity and segregation determination using NIR spectroscopy, Colloid Surf. A-
574 Physicochem. Eng. Asp., 288 (2006) 71-76.

575 [34] J. Johansson, S. Pettersson, S. Folestad, Characterization of different laser irradiation
576 methods for quantitative Raman tablet assessment, J. Pharm. Biomed. Anal., 39 (2005)
577 510-516.

578 [35] Y. Xie, W. Tao, H. Morrison, R. Chiu, J. Jona, J. Fang, N. Cauchon, Quantitative
579 determination of solid-state forms of a pharmaceutical development compound in drug
580 substance and tablets, Int. J. Pharm., 362 (2008) 29-36.

581 [36] H. Wikström, I.R. Lewis, L.S. Taylor, Comparison of sampling techniques for in-
582 line monitoring using Raman spectroscopy, Appl. Spectrosc., 59 (2005) 934-941.

583 [37] Y. Hu, H. Wikström, S.R. Byrn, L.S. Taylor, Analysis of the effect of particle size
584 on polymorphic quantitation by Raman spectroscopy, Appl. Spectrosc., 60 (2006) 977-
585 984.

586 [38] M.V. Schulmerich, W.F. Finney, R.A. Fredricks, M.D. Morris, Subsurface Raman
587 spectroscopy and mapping using a globally illuminated non-confocal fiber-optic array
588 probe in the presence of Raman photon migration, Appl. Spectrosc., 60 (2006) 109-114.

589 [39] J. Rantanen, H. Wikström, F.E. Rhea, L.S. Taylor, Improved understanding of
590 factors contributing to quantification of anhydrate/hydrate powder mixtures, Appl.
591 Spectrosc., 59 (2005) 942-951.

592 [40] H.L. Wang, C.K. Mann, T.J. Vickers, Effect of powder properties on the intensity of
593 Raman scattering by crystalline solids, Appl. Spectrosc., 56 (2002) 1538-1544.

594 [41] P. Allan, L.J. Bellamy, A. Nordon, D. Littlejohn, Non-invasive monitoring of the
595 mixing of pharmaceutical powders by broadband acoustic emission, Analyst, 135 (2010)
596 518-524.

597 [42] R.C. Rowe, P.J. Sheskey, P.J. Weller, Handbook of Pharmaceutical Excipients, 4th
598 ed., Pharmaceutical Press, London, 2003.

599 [43] F.C. Clarke, S.V. Hammond, R.D. Jee, A.C. Moffat, Determination of the
600 information depth and sample size for the analysis of pharmaceutical materials using
601 reflectance near-infrared microscopy, Appl. Spectrosc., 56 (2002) 1475-1483.

602 [44] O. Berntsson, L.G. Danielsson, S. Folestad, Estimation of effective sample size
603 when analysing powders with diffuse reflectance near-infrared spectrometry, Anal. Chim.
604 Acta, 364 (1998) 243-251.

605 [45] U. Balachandran, N.G. Eror, Raman spectra of titanium dioxide, J. Solid State
606 Chem., 42 (1982) 276-282.

607 [46] B. Schrader, G. Bergmann, Die intensität des Ramanspektrums polykristalliner
608 substanzen I. Strahlingsbilanz von substanz und probenanordnung, Z. Anal. Chem. Fres.,
609 225 (1967) 230-247.

610 [47] B. Schrader, A. Hoffmann, S. Keller, Near-infrared Fourier-transform Raman
611 spectroscopy - facing absorption and background, Spectrochim. Acta, 47A (1991) 1135-
612 1148.

613 [48] O. Berntsson, T. Burger, S. Folestad, L.G. Danielsson, J. Kuhn, J. Fricke, Effective
614 sample size in diffuse reflectance near-IR spectrometry, Anal. Chem., 71 (1999) 617-623.

615 [49] N. Everall, T. Hahn, P. Matousek, A.W. Parker, M. Towrie, Picosecond time-
616 resolved Raman spectroscopy of solids: Capabilities and limitations for fluorescence
617 rejection and the influence of diffuse reflectance, Appl. Spectrosc., 55 (2001) 1701-1708.

618 [50] N. Everall, T. Hahn, P. Matousek, A.W. Parker, M. Towrie, Photon migration in
619 Raman spectroscopy, Appl. Spectrosc., 58 (2004) 591-597.

620 [51] M.V. Pellow-Jarman, P.J. Hendra, R.J. Lehnert, The dependence of Raman signal
621 intensity on particle size for crystal powders, Vib. Spectrosc., 12 (1996) 257-261.

622 [52] H. Owen, D.J. Strachan, J.B. Slater, J.M. Tedesco, Large-collection-area optical
623 probe, US Pat., WO2005060622 A2, 2005.
624
625
626

Table captions

Table 1. Detection limit for aspirin in Avicel PH-101 mixing at 50 rpm for non-invasive NIR spectrometry, acoustic emission (AE) and Raman spectrometry.

Technique	Signal	Detection limit/(% w/w)[a]
NIR	1st derivative of log(1/R) at 8956 cm^{-1}	0.1
Raman	2nd derivative at 1606 cm^{-1}	1.1
AE	Area between 0 and 400 kHz	5.2

[a] Detection limit calculated from 3 times the standard deviation of the signal between 702 and 900 s in the mixing profile for Avicel PH-101 alone (n = 34) divided by the sensitivity of the signal response for aspirin. The sensitivity was obtained from a plot of concentration (0 –28.6% w/w for AE and 0 –34.8% w/w for NIR and Raman) against average signal intensity between 702 and 900 s in the mixing profiles (n = 34). The NIR and Raman data were resampled to match the acquisition frequency of the AE measurements (every 6 s).

641 **Figure captions**

642 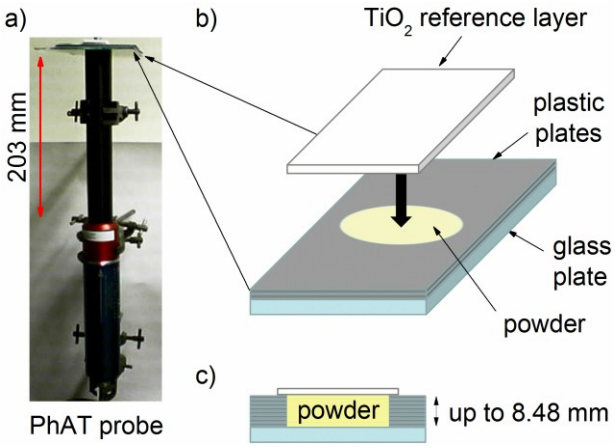

643 Figure 1. a) Raman PhAT probe set up for sampling depth experiments with powders, b)
644 expansion of sample set up showing the glass plate, plastic plates and TiO_2 reference
645 layer, and c) end on view of sample set up.

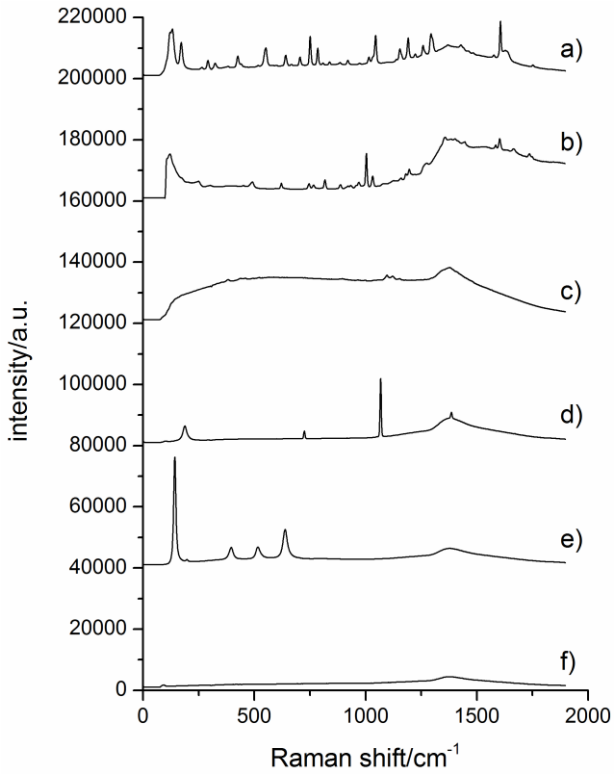

Figure 2. Offset Raman spectra of a) aspirin, b) aspartame, c) Avicel PH-101, d) sodium nitrate, e) TiO_2 reference layer (intensity reduced by a factor of 4) and f) 2.68 mm thick glass plate. All spectra, except for aspartame, were acquired using the PhAT probe with an exposure time of 0.5 s and 1 accumulation. The spectrum for aspartame was acquired using a MR probe with an exposure time of 4.0 s and 1 accumulation.

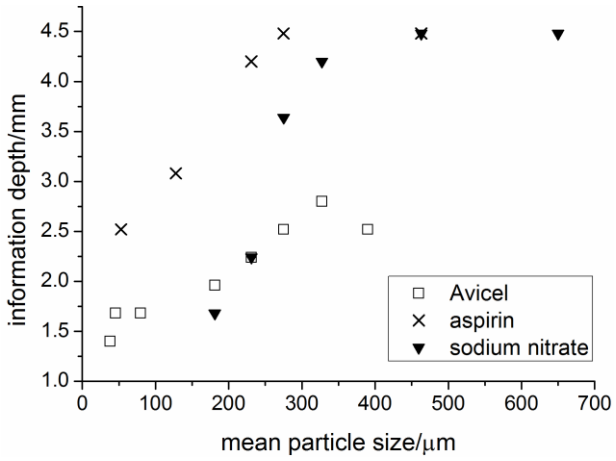

653

654 Figure 3. Information depths of Avicel, aspirin and sodium nitrate of different particle

655 sizes, based on measurements of the TiO_2 peak at 397 cm^{-1}.

656

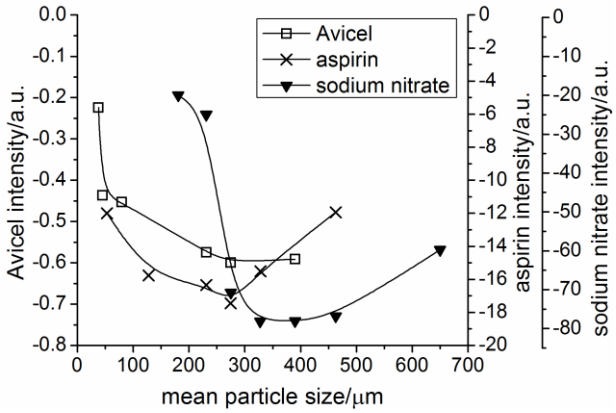

657

658 Figure 4. Second derivative Raman signal intensity for measurements at aspirin
659 (1606 cm^{-1}), Avicel (1095 cm^{-1}) and sodium nitrate (1068 cm^{-1}) peaks for increasing
660 particle size ranges with a powder depth of 8.48 mm. The lines drawn through the data
661 points were calculated using a cubic B-spline function.

662

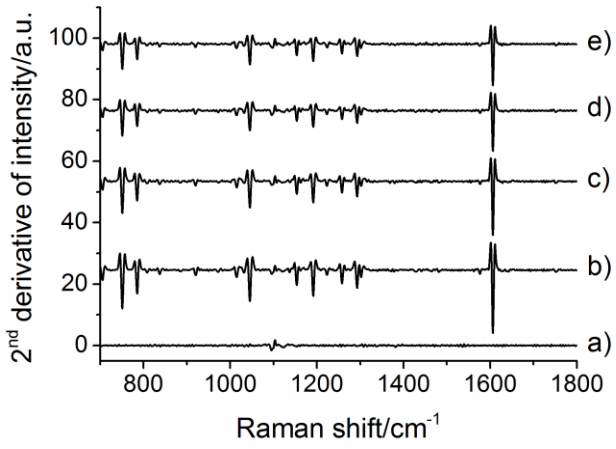

663

664 Figure 5. Offset second derivative Raman spectra obtained at a) 50, b) 150, c) 200, d) 400
665 and e) 800 s during the mixing of 40 g of aspirin (particle size range 250 – 300 μm) and
666 Avicel PH-101. Aspirin was added to Avicel at 120 s and a mixing speed of 50 rpm was
667 used.

668

669 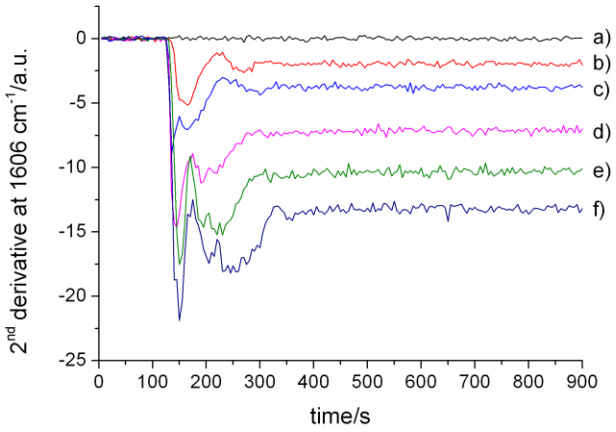

670 Figure 6. Raman PhAT probe mixing profiles at 1606 cm^{-1} for additions of a) 0, b) 5, c)
671 10, d) 20, e) 30 and f) 40 g of aspirin (particle size range 250 – 300 μm) to Avicel PH-
672 101 at 120 s, mixing with an impeller speed of 50 rpm.

673

674 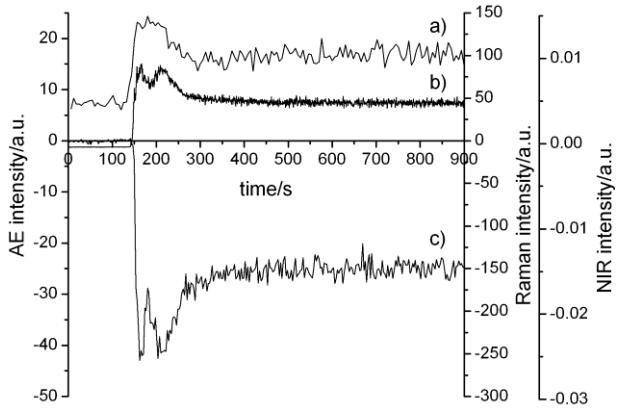

675 Figure 7. Mixing profiles for addition of 30 g aspirin to 75 g Avicel PH-101 at 120 s
676 mixing at 50 rpm, obtained simultaneously by three non-invasive techniques: a) acoustic
677 emission spectrometry (area between 0 and 400 kHz); b) NIR spectrometry (1st derivative
678 of log(1/R) at 8956 cm^{-1}), and c) Raman spectrometry (2nd derivative of intensity at
679 1606 cm^{-1}).

680

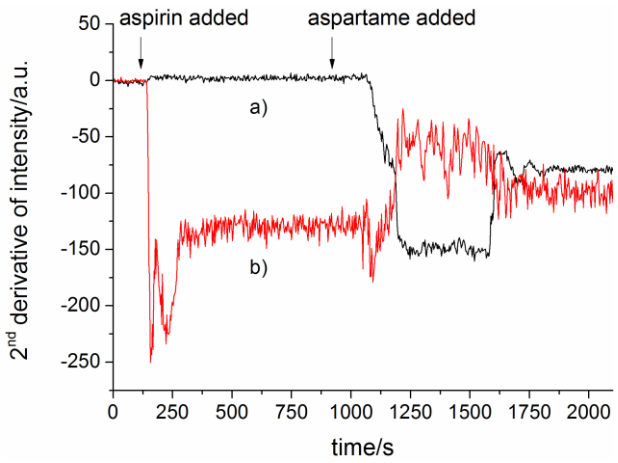

681

682 Figure 8. Raman mixing profiles obtained using a) the aspartame peak at 1006 cm^{-1} and

683 b) the aspirin peak at 1606 cm^{-1} for addition of 25 g aspirin (120 s) and 25 g aspartame

684 (900 s) to 75 g Avicel PH-101 mixing at 50 rpm.